JOURNAL OF SOLID STATE CHEMISTRY 3, 323–339 (1971)

Phase Equilibria and Structural Relations in the System $BaMnO_{3-x}$

T. NEGAS AND R. S. ROTH

National Bureau of Standards, Washington, D.C. 20234

Received October 9, 1970

The system $BaMnO_{3-x}$ ($0 \leqslant x < 0.5$) in air was investigated by gravimetric, quenching, single-crystal and powder-X-ray diffraction studies. Below 1150°C hexagonal, two-layer $BaMnO_3$ ($a = 5.699$ Å, $c = 4.817$ Å) is stable. Above 1150°C a series of anion deficient $BaMnO_{3-x}$ phases exists. With increasing temperature, these include a rhombohedral 15-layer form ($a = 5.681$ Å, $c = 35.377$ Å; hexagonal indexing) and hexagonal 8-layer ($a = 5.699$ Å, $c = 18.767$ Å), 6-layer ($a = 5.683$ Å, $c = 14.096$ Å), 10-layer ($a = 5.680$ Å, $c = 23.373$ Å) and 4-layer ($a = 5.672$ Å, $c = 9.319$ Å) forms. The 6-layer modification is not of the hexagonal $BaTiO_3$-type. A simple orderly structural sequence involving a progressive increase of cubic-type layer stacking with increasing temperature characterizes the phases prepared. Influence of anion stoichiometry on phase formation is considered.

Introduction

Mixed metal oxides of the type XYO_3 (X = large cations, Ba, Sr, Ca; Y = transition metals) have been extensively studied from a crystallochemical standpoint because of their interesting physical properties. These materials basically consist of a stacking of close-packed XO_3 layers with transition metals occupying interlayer octahedral sites. Based on the number of layers, the stacking sequence, and ordering of transition metals, numerous unique structure types theoretically can be generated. Some have been realized experimentally. These are well-summarized by Katz and Ward (*1*). A detailed discussion of the stacking of close-packed units, generated symmetry, and descriptive Zhdanov notation is provided in the "International Tables for X-ray Crystallography" (*2*).

All of these structure types can be considered to consist of mixtures of two types of layer packing. Total hexagonal stacking (ABAB, every other layer is identical) of XO_3 layers results in a two-layer hexagonal cell (hex 2L, L = layer) characterized by infinite strings of face-sharing transition metal-oxygen octahedra parallel to the c axis. The compound $BaNiO_3$ (*3*) is a frequently cited example although its oxygen stoichiometry remains questionable. Total cubic stacking (ABC, neighboring layers unlike) yields the familiar perovskite structure in which all octahedra share corners. An alteration of face- and corner-sharing octahedra results from mixed cubic and hexagonal stacking. Hexagonal, 6L $BaTiO_3$ (ABCACB) with $66\frac{2}{3}\%$ cubic stacking (*4*) and hexagonal, 4L $SrMnO_3$ (ABAC) with 50% cubic stacking (*5*, *6*) are typical.

Barium manganese oxides (Ba/Mn = 1:1) were prepared by Gushee et al. (*7*), Hardy (*8*), and Donohue et al. (*9*). Gushee et al. prepared at 900 and 1000°C in air a nearly homogeneous hexagonal phase with $a = 5.7$ Å and $c = 4.8$ Å, apparently isostructural with hex 2L "$BaNiO_3$" and $BaCoO_{2.85}$ (*7*). Hardy prepared a hex 2L, $a = 5.672$ Å and $c = 4.71$ Å, $BaMnO_3$ by heating $BaMnO_4$ near 400°C. Above 1150°C, a hex 4L "$BaMnO_3$" with $a = 5.669$ Å and $c = 9.375$ Å was synthesized in argon (*8*). Donohue et al. reported a rhombohedral 9L form with $a = 5.662$ Å and $c = 20.915$ Å obtained from a BaO_2: MnO_2 mixture heated in air at 1000°C. The phase could not be duplicated but could be stabilized with as little as 5 mole % ruthenium. Recently, Negas et al. (*5*) described a number of other modifications prepared at elevated temperatures in air. They suggested that these were not stoichiometric $BaMnO_3$ phases but tended to be oxygen deficient. Chamberland et al. (*10*) prepared the hex 2L form, a rhombohedral 9L modification (at elevated pressures), and a nonstoichiometric 4L phase.

This paper describes the preparation, phase relations, and crystallographic features of a number of single-phase barium–manganese oxides. The con-

ditions of preparation yield entirely reproducible products. Their stability, reversibility, and probable stoichiometry are considered.

Experimental Procedure

Various combinations of starting reactants were used. These include reagent grade and spectrographic grade $BaCO_3$, spectrographic grade $Ba(NO_3)_2$, two commercial sources of reagent grade MnO_2, and spectrographic grade MnO_2. Spectrochemical analyses for both the high purity $BaCO_3$ and $Ba(NO_3)_2$ show: Ca, Mg <1 ppm; all others below limits of detection. Spectrochemical analyses for the MnO_2 show: reagent grade MnO_2: Ag <0.001; Ca <0.001; Cr, Cu, Fe, Ni, Sn, Zn, 0.001–0.01; in wt %; high purity MnO_2: Fe, Si, 2 ppm; Ca, Cu, 1 ppm; Mg <1 ppm. A limited number of experiments were conducted using $BaMnO_4$, prepared by the Analytical Section at NBS, and $BaMn_2O_8$. Weighed amounts of the appropriate starting materials were hand mixed under acetone, packed in gold envelopes, and calcined in air for about 2 weeks at 800°C followed by an additional 2 weeks at 1000°C. Calcined, single-phase specimens were equilibrated in air using the quench method. A number of heatings were conducted in vacuum and in flowing argon. A vertical tube resistance-type furnace was used for heatings while specimens were quenched in either solid CO_2, liquid nitrogen, water, or on a cold metal tray. Temperatures were measured with Pt–Pt 10% Rh thermocouples calibrated, under conditions simulating the heating of a specimen, against the melting points of NaCl, Au, and Pd. The quench furnaces were controlled by an a-c Wheatstone bridge instrument capable of maintaining temperature to at least ± 2°C.

Gravimetric data were obtained generally from 1.5–2.0-g specimens, which were previously equilibrated at a desired temperature and quenched. These specimens were weighed at room temperature then heated in air to about 1000°C. The specimens were removed from the furnace after permitting enough time for any weight changes to occur and reweighed after cooling. Unless otherwise indicated, all measurements involve a weight gain from a high-temperature phase to a low-temperature oxidized phase.

X-ray powder patterns of specimens were made at room temperature using a high-angle Geiger counter diffractometer and Ni-filtered Cu radiation. The scanning rate was $1/4°2\theta$/min. Unit cell dimensions were refined by a least-squares computer program and are estimated to be accurate to at least ± 2 in the last decimal place listed. Single-crystal X-ray photographs were taken with a precession camera. Quantitative intensity data for one of the phases were collected on an automatic diffractometer with Cu K_α radiation. Computer programs from "X-ray 67, Program System for X-ray Crystallography" (*11*) were used for the structure analysis and least-squares refinement. Powder-pattern intensity calculations were made using the program of Smith (*12*).

Experimental Results and Discussion

The air (ambient pressure) isobar in the system $BaMnO_{3-x}$ between $x=0$ to $x=0.50$ is shown in Fig. 1. The diagram was constructed from the quenching and gravimetric data in Table I. All data in Table I are not indicated in Fig. 1 for purposes of clarity. Results are expressed in terms of the formula $BaMn^{3+}_{2x}Mn^{4+}_{1-2x}O_{3-x}$ as Mn^{3+} is compatible with trigonal bipyramidal coordination resulting from oxygen loss.

Two-Layer Modification

Below approximately 1150°C in air, a homogeneous, yellow-green (in fine-powder form) material can be prepared. Its X-ray powder pattern, given in Table II, is indexed on the basis of a hexagonal cell with $a=5.699$ Å and $c=4.817$ Å. Unit cell parameters are similar to those given by Hardy (*8*) and nearly identical to those of Chamber-

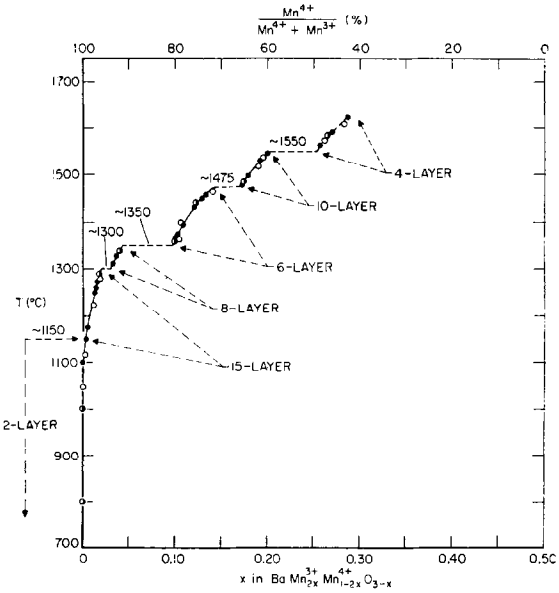

FIG. 1. Phase relations in air in the system $BaMnO_{3-x}$. ●, Single-phase solid; ○, single-phase solid where x was determined gravimetrically; ◑ combination of the above.

TABLE I

EXPERIMENTAL DATA FOR THE SYSTEM $BaMnO_{3-x}$

Starting material[a]	Treatment[b] Time (hr)	Temp. (°C)	Special conditions[d]	Products and comments[c]	Composition x in $BaMnO_{3-x}$
2L	335	800		2L	0.00
	335	1000		2L; in both Pt and Au	0.00
	15	1000		15L + 8L; reheat of 1320°C specimen	
	120	1000		15L + 8L; reheat of 1320°C specimen	
	240	1010	OX	2L	
	335	1045		2L; in both Pt and Au	0.00
	89	1100		2L	
	192	1100	S.T.	15L crystals + 2L	
	16	1150		2L	
	16	1175		2L + 15L	
	170	1175		15L	
	0.25	1200		2L, metastable	
	1	1200		2L, metastable	
	86	1250		15L	
	65	1250		15L + tr. 2L	
	336	1250		8L + 15L; reheat of 1312°C specimen	
	144	1250	S.T.	8L crystals	
	144	1260		15L	
	72	1285		15L	
	72	1285	OX	15L	
	144	1290		15L	
	212	1312		8L + 15L	
	144	1318		8L + 15L	
	144	1319		8L + 15L	
	4	1320		15L + 8L	
	168	1321		8L + 15L	
	312	1328		8L; reheat of 1321°C specimen	
	168	1335		8L; reheat of 1341°C specimen	
	432	1339		8L; reheat of 1312°C specimen	0.041
	120	1341		8L + 15L; reheat of 1312°C specimen	
	120	1341		8L + 15L	
	16	1350	S.T.	8L	
	144	1360		6L	0.100
	96	1360		6L	
	120	1375		6L	
	48	1375	S.T.	8L	
	48	1375	S.T.	8L + 6L; leaked	
	65	1395		6L	
	48	1430	S.T.	6L	
	216	1432		6L	
	16	1450		6L	
	24	1460		6L	
	16	1485		10L	
	72	1497		10L	
	1	1530		10L	
	17	1545		10L	
	6	1560		4L	
	2	1562		4L	
	24	1580		4L + tr. "X"[e]	

TABLE I—*continued*

Starting material[a]	Treatment[b] Time (hr)	Temp. (°C)	Special conditions[d]	Products and comments[c]	Composition x in $BaMnO_{3-x}$
2L—*continued*	6	1585		4L	0.265
	12	1585		4L + tr. "X"	
	7	1590		4L + tr. "X"	
	24	1610		4L + tr. "X"	
	168	1000		Unidentified phases; reheat of 1350°C, 70-μ vacuum specimen	
	65	1250	350 μ V	4L + tr. "Y"[f]	
	16	1275	10 μ V	4L + "Y"	
	144	1350	250 μ V	"Y" + 4L	
	240	1350	70 μ V	"Y"	
	72	1400	100 μ V	"Y"; reheat of 1350°C, 250-μ specimen	
	72	1400	150 μ V	4L + tr. "Y"	
	72	1400	150 μ V; mixed with PtO_2	"Y" + tr. 4L	
	96	1407	150 μ V; ~3 g	4L + "Y"	
	24	1580		"X"; reheat of 1350°C, 70-μ specimen	
	2	1627		"X"; reheat of 1400°C, 100-μ specimen	
	168	~1150	A	6L + tr. 15L	
	45	~1300	A	4L + tr. "Y"	
15L	336	1000	S.T.	15L	
	1344	1000		15L, no reversal to 2L	
	144	1116		15L	0.003
	167	1226		15L	0.012
	170	1280		15L	0.019
	332	1291		15L	0.018
	144	1300	S.T.	15L	
	144	1319		15L + tr. 8L	
	100	1335		15L + tr. 8L	
	100	1340		15L + tr. (?) 8L; in field of 8L	0.040
	120	1341		15L + 8L	
	96	1363		6L	0.104
	120	1366		6L	
	96	1401		6L	0.107
	96	1442		6L	0.123
	216	1442		6L	
	240	1451		6L	
	120	1464		6L	0.141
	120	1478		10L	
	72	1485		10L	0.174
	96	1519		10L	0.190
	96	1537		10L	0.195
	5	1573		4L	0.262
	24	1573		4L + tr. "X"	
	8	1608		4L	0.283
	45	1300	A	4L + tr. "Y"	
8L	336	1000	S.T.	8L	
	192	1000		8L, no reversal to 2L	
	336	1252		8L, no reversal to 15L	
	240	1365		6L	

TABLE I—*continued*

Starting material[a]	Treatment[b] Time (hr)	Temp. (°C)	Special conditions[d]	Products and comments[c]	Composition x in $BaMnO_{3-x}$
8L—*continued*	120	1478		10L	
	2	1562		4L	
6L	336	1000	S.T.	6L	
	336	1000		2L	
	216	1253	S.T.	6L	
	216	1253		15L	
	168	1321		8L + 15L	
	312	1328		8L, reheat of 1321°C specimen	
	120	1366		6L	
	216	1442		6L	
	240	1451		6L	
	120	1478		6L + tr. 10L	
	2	1562		4L	
	168	~1150	A	6L	
	45	~1300	A	4L + tr. "Y"	
10L	336	800		2L + 15L	
	336	1000		2L + 15L	
	1344	1000		2L + 15L	
	336	1000	S.T.	10L	
	216	1253		15L	
	144	1300	S.T.	10L	
	168	1321		8L + 15L	
	312	1328		8L + tr. 15L; reheat of 1321°C specimen	
	120	1366		6L	
	216	1442		6L	
	240	1451		6L	
	120	1478		10L	
	2	1562		4L	
	168	~1150	A	6L + tr. 15L	
	45	~1300	A	4L + tr. "Y"	
4L	336	1000	S.T.	4L	
	103	1000		2L	
	240	1010	OX	2L	
	216	1253		15L	
	144	1300	S.T.	4L	
	168	1321		8L + 15L	
	312	1328		8L; reheat of 1321°C specimen	
	120	1366		6L	
	216	1442		6L	
	240	1451		6L	
	120	1478		10L	
	2	1623		4L + tr. "X"	
	17	1626		4L + "X", reheat of 1623°C specimen	
	1	1630		Partly melted 4L + "X"	
	1	1642		Melted "X" + 4L	
	168	~1150	A	6L + tr. 15L	
	72	~1250	A	4L + tr. "Y"	
	45	~1300	A	4L + tr. "Y"	
1:2 (Ba:Mn)	22	1000		2L + Mn-rich phase	
	24	1100		2L + Mn-rich phase	
	216	1253		15L + Mn_3O_4	

TABLE I—*continued*

Starting material[a]	Treatment[b] Time (hr)	Temp. (°C)	Special conditions[d]	Products and comments[c]	Composition x in $BaMnO_{3-x}$
1:2(Ba:Mn)— *continued*	120	1366		6L + Mn_3O_4	
	216	1442		Partly melted; 6L + Mn_3O_4	
	72	1325	150 μ V	4L + MnO	
	72	1345	4 μ V	4L + MnO	
	96	1420	150 μ V	Partly melted; 4L + unidentified phase	
1:6 (Ba:Mn)	96	1000		Unidentified phase (see 1:2, 1000 and 1100°C) + Mn_3O_4	
$BaMnO_4$	24	500		2L	
	120	1000		2L	
	216	1253		15L	
	120	1366		6L	
	216	1442		6L	
	240	1451		6L	
	120	1478		10L	
	6	1565		4L	

[a] 2L = two-layer phase, 15L = fifteen-layer phase, 8L = eight-layer phase, 6L = six-layer phase, 10L = ten-layer phase, 4L = four-layer phase.

[b] Unless otherwise indicated heatings were conducted in air in Pt or Au containers.

[c] Determined by X-ray powder diffraction analysis. The predominant phase is given first, tr. = trace.

[d] OX—in 1 atmosphere oxygen, S.T.—in sealed Pt tube, V—in vacuum, A—in argon; partial pressure of oxygen unknown.

[e] "X" = Ba-rich, unidentified phase.

[f] "Y" = Ba-rich, unidentified phase similar to "X".

land et al. (*10*) for stoichiometric 2L $BaMnO_3$. The structure of this compound is reported to consist of a two-layer sequence (AB, 100% hexagonal stacking) of BaO_3 layers with continuous strings of face-sharing manganese–oxygen octahedra parallel to the c axis.

The 2L phase was prepared from a variety of starting materials including $BaMnO_4$, $BaCO_3 + BaMn_2O_8$, $Ba_3Mn_2O_8 + MnO_2$, $Ba_3Mn_2O_8 + Mn_3O_4$, $BaCO_3 + MnO_2$ and $Ba(NO_3)_2 + MnO_2$. Two-layer material, prepared from reactions involving a carbonate was examined at room and liquid nitrogen temperatures with infrared. Carbonate, hydroxyl, and H_2O groups were not detected. Regardless of the starting materials, the final products from all reactions are identical. Furthermore, the results of experiments conducted at elevated temperatures using 2L starting material are insensitive to the previous chemical and thermal history of the 2L phase. Material obtained from an independent source (*10*) yielded identical results.

Two-layer material can be synthesized with the greatest facility by heating $BaMnO_4$ above 400°C in air. Short firing times (<1 day) and/or low temperatures (< 800°C) produce a very poorly crystalline phase whose X-ray pattern is characterized by broad, weak lines, particularly those with indices other than ($hk0$) and ($h00$). Prolonged heating (>1 week) between 800–1100°C or short term (1–2 hr) firing between 1200–1275°C (within the temperature stability range of a different modification and, therefore, metastably) yields 2L material with substantially better crystallinity. Regardless of the heat treatment, X-ray patterns never quite have that excellent quality normally associated with well-ordered crystalline phases.

Although the two-layer phase was shown to be stoichiometric $BaMnO_3$ (*8*), attempts were made to study gravimetrically several reactions which could confirm independently the oxygen content and thereby establish a compositional reference point for subsequent experiments. Inconsistent data were obtained by reducing $BaMnO_4$ at 1000°C in air. The "$BaMnO_4$" used in this study apparently contains H_2O as it is violet and has cell parameters roughly 0.5% larger than those reported by Jellinek (*13*) for the pure form.

However, the reaction,

$$(1)\quad Ba_3Mn_2O_8 + MnO_2 \xrightarrow[\text{air, 164 hr}]{1000^\circ C} Ba_3Mn_3O_{10-x} + x0,$$

TABLE II

X-RAY DIFFRACTION DATA FOR TWO-LAYER $BaMnO_3$

d_{obsd}	d_{calcd}	$h\,k\,l^a$	I_{obsd}
3.446	3.447	1 0 1	78
2.849	2.850	1 1 0	100
2.467	2.468	2 0 0	3
2.407	2.408	0 0 2	9
2.196	2.196	2 0 1	60
2.164	2.164	1 0 2	29
1.8399	1.8394	1 1 2	6
1.7394	1.7397	2 1 1	24
1.7236	1.7236	2 0 2	18
1.6453	1.6453	3 0 0	17
1.5267	1.5268	1 0 3	6
1.4748	1.4748	2 1 2	15
1.4248	1.4249	2 2 0	18
1.3587	1.3585	3 0 2	2
1.3459	1.3458	2 0 3	6
1.3170	1.3168	3 1 1	9
1.2263	1.2263	2 2 2	2
1.2169	1.2169	2 1 3	3
1.2042	1.2041	0 0 4	2
1.1952	1.1954	4 0 1	7
1.1902	1.1901	3 1 2	6
1.1091	1.1092	1 1 4	6
1.1024	1.1023	3 2 1	7
1.0771	1.0771	4 1 0	8

[a] Indexed on the basis of a hexagonal cell with $a = 5.699$ Å and $c = 4.817$ Å.

gave a 2.24% weight loss corresponding to $x = 1.03$ and a composition near $BaMnO_{2.99}$. The emerald-green phase $Ba_3Mn_2O_8$, isostructural with $Ba_3P_2O_8$ (*14*), was prepared at 800°C in air from $BaCO_3$ and MnO_2. It has hexagonal cell parameters $a = 5.713$ Å and $c = 21.453$ Å.

Fifteen-Layer Modification

With prolonged heating (at least 5 days) between 1150 and 1300°C, the 2L phase transforms to a new modification. The powder pattern of this dark-brown (in fine powder form) phase is of excellent quality. Although rhombohedral, it is indexed on the basis of a hexagonal cell with $a = 5.681$ Å and $c = 35.377$ Å in Table III. Assuming an average thickness of approximately 2.35–2.40 Å for a BaO_3 layer, the c dimension suggests a 15-layer stacking sequence. If the 2L phase is heated for short time intervals at the lower portion of the temperature range indicated above, a two-phase mixture consisting of the 2L plus a 15L-like phase results initially. The diffraction pattern of the latter contains diffuse (*hkl*) but sharp (*h*00) and (*hk*0) lines suggesting a tendency toward ordering of BaO_3 layers perpendicular to c. Single-phase, well-crystallized material results from continued heating. This reaction sequence is clearly demonstrated by pertinent powder pattern segments in Fig. 2.

Although 2L material, on heating above 1150°C, converts to 15L, reversal does not occur. For example, heating the 15L phase for 8 weeks at 1000°C in air showed not even a tendency toward reversal to 2L. Weight changes are measurable,

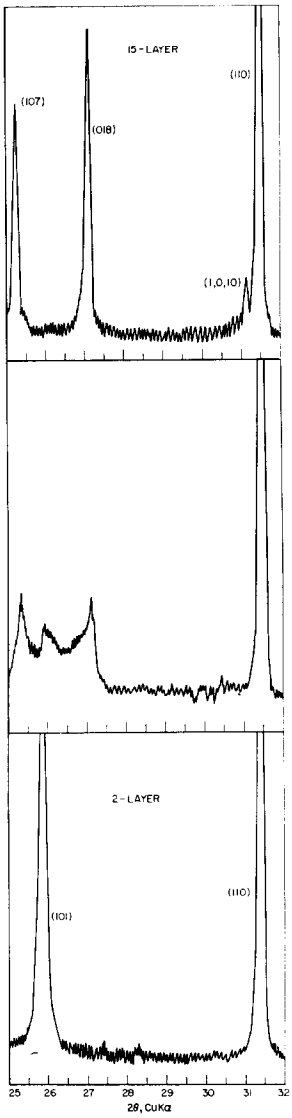

FIG. 2. Portions of powder patterns which depict the transformation of two-layer $BaMnO_3$ to a 15-layer modification. Bottom: two-layer phase; middle: material heated 16 hr, 1175°C, in air; top: material heated 170 hr, 1175°C, in air.

TABLE III

X-RAY DIFFRACTION DATA FOR FIFTEEN-LAYER $BaMnO_{3-x}$

d_{obsd}	d_{calcd}	$h\ k\ l$[a]	I_{obsd}	I^b_{calcd}	I^c_{calcd}	I^d_{calcd}
3.526	3.525	1 0 7	35	48	53	58
3.290	3.290	0 1 8	50	63	63	63
2.872	2.872	1,0,10	8	8	8	5
2.840	2.841	1 1 0	100	100	100	100
2.692	2.692	0,1,11	2	2	2	3
2.454	2.454	0 2 1	3	3	<1	<1
2.382	2.381	1,0,13	5	6	7	5
2.359	2.358	0,0,15	12	11	4	4
2.324	2.324	2 0 5	2	1	<1	<1
2.248	2.248	0,1,14	9	14	15	15
2.212	2.212	0 2 7	28	31	13	14
2.149	2.150	2 0 8	39	35	17	17
2.018	2.020 2.017	0,2,10 1,0,16	9	10	10	10
1.9541	1.9540	2,0,11	2	2	<1	1
1.8254	1.8249	0,2,13	7	4	3	2
1.8148	1.8146	1,1,15	9	8	9	9
1.7631	1.7627	2,0,14	9	11	6	6
1.7453	1.7453	2 1 7	11	9	11	12
1.7146	1.7143	1 2 8	15	14	16	16
1.6448	1.6445	0,2,16	8	9	6	6
1.6405	1.6401	3 0 0	25	20	18	18
1.5352	1.5354	2,1,13	3	4	3	2
1.5283	1.5285	1,0,22	4	5	4	5
1.4980	1.4978	1,2,14	9	8	7	7
1.4680	1.4681	0,1,23	3	4	4	3
1.4231	1.4232	2,1,16	8	8	6	6
1.4204	1.4204	2 2 0	22	17	11	11
1.3460	1.3465 1.3460	3,0,15 0,2,22	6	7	5	5
1.3174	1.3174	1 3 7	6	4	4	4
1.3040	1.3042 1.3039	2,0,23 3 1 8	10	10	7	7
1.2166	1.2167 1.2164	2,2,15 2,1,22	8	7	5	6
1.2007	1.2007	3,1,14	3	3	3	3
1.1952	1.1952	4 0 7	3	2	1	1
1.1849	1.1852 1.1851	1,2,23 0 4 8	5	6	5	4
1.1792	1.1792	0,0,30	3	2	1	2
1.1015	1.1016	3 2 7	2	2	2	2
1.0936	1.0937	2 3 8	4	3	3	3
1.0891	1.0891	1,1,30	4			
1.0750	1.0754 1.0749	3,2,10 4,0,16	3			
1.0737	1.0737	4 1 0	9			

[a] Indexed on the basis of hexagonal cell with $a = 5.681$ Å and $c = 35.377$ Å. The phase is rhombohedral.

[b] Calculated on the basis of a fifteen-layer structure with $R\bar{3}m$ symmetry. The structure was refined with single-crystal intensity data to $R = 10.2$ (1378 independent reflections). Refined positional parameters are: 3 Ba at (*a*), 6 Ba at (*c*), $z = 0.1337$, 6 Ba at (*c*), $z = 0.2650$; 9 O at (*e*), 18 O at (*h*), $x = 0.1856$, $z = 0.0640$, 18 O at (*h*), $x = 0.4835$, $z = 0.1330$; 3 Mn at (*b*), 6 Mn at (*c*), $z = 0.3613$, 6 Mn at (*c*), $z = 0.4315$.

[c] Same as footnote (*b*) but excluding oxygens.

[d] Calculated on the basis of an ideal fifteen-layer structure with $R\bar{3}m$ symmetry. Oxygens are excluded. Atomic parameters used are: 3 Ba at (*a*), 6 Ba at (*c*), $z \approx 2/15$ (0.1333), 6 Ba at (*c*), $z \approx 4/15$ (0.2667); 3 Mn at (*b*), 6 Mn at (*c*), $z \approx 11/30$ (0.3667), 6 Mn at (*c*), $z \approx 13/30$ (0.4333).

however. In Fig. 1, the curve showing the deviation from $BaMnO_3$ stoichiometry of 15L was derived from weight-regain data and calculations associated with the general reaction:

$$\underset{15L}{BaMnO_{3-x}} + x0 \xrightarrow[air]{1000^\circ C} \underset{15L}{BaMnO_3}. \quad (2)$$

Precalcined (1250°C, 2 weeks) 15L, equilibrated and quenched from a given temperature within the 1100–1300°C range constituted the $BaMnO_{3-x}$ of Eq. (2). The value of x was then calculated assuming that the final bulk composition after a weight gain at 1000°C is stoichiometric $BaMnO_3$ even though reversal to 2L does not occur. It remains unclear, however, whether (a) the 15L phase exists only metastably below 1150°C; (b) a true polytypic or disorder–order relationship exists between 2L and 15L, or (c) a small amount of reduction is absolutely required before 15L can form from 2L. As shown in Fig. 1, the 15L phase exists within the composition range $x = 0$ to approximately $x = 0.02$. Cell parameter variation or cell distortion from apparent rhombohedral symmetry with stoichiometry are not evident.

Small single crystals (< 0.1 mm) of the 15L phase were unusually easy to grow. A few milligrams of the 2L phase were sealed in a 3/4 in. flattened Pt tube, heated at 1100°C for 192 hr and quenched. Black hexagonal platelets, some twinned, grew in a matrix consisting of 2L material. In air at this same temperature, the 2L to 15L conversion was not observed. Increased pressure due to trapped air and/or oxygen generated from the specimen probably enhanced transformation and crystal growth. After heating, the sealed tubes showed obvious swelling. Single-crystal precession data confirmed the *c*-axis multiplicity and the *a* dimension obtained from powder data. The X-ray data are consistent with the space groups $R32$, $R3m$, and $R\bar{3}m$. Using intensity data collected with an automatic diffractometer, a partial solution of the three-dimensional Patterson function followed by three-dimensional F_{obsd} and F_{diff} maps, all calculated by the use of

"X-ray 67, Program System for X-ray Crystallography" (*11*), yielded a basic structure. Based on $R\bar{3}m$ symmetry, $Ba_{15}Mn_{15}O_{45}$ stoichiometry and 1378 independent reflections, the structure was refined (least-squares program, "X-ray 67") to $R = 10.2\%$. All isotropic temperature factors are positive. Without oxygens, $R = 14.3\%$. Details of the structural analysis will be published with N. C. Stephenson elsewhere. Final atomic parameters are given in Table III. Three sets of powder-pattern intensity calculations were made using the program of Smith (*12*). These, also given in Table III, include calculated intensities based on (a) refined atomic parameters derived from single-crystal data and $Ba_{15}Mn_{15}O_{45}$ stoichiometry, (b) refined atomic parameters with oxygen excluded, and (c) ideal atomic parameters excluding oxygen. The intensities calculated for all three cases are in good agreement with those observed. It, therefore, appeared possible to deduce the structures of the other phases in this study by using ideal atomic parameters derived from packing considerations. Furthermore, it is demonstrated that possible oxygen deficiency has a marginal effect on the intensities. The structure of the 15L phase is shown in Fig. 3. It consists of strings of five face-sharing octahedra linked by corner sharing within the cubically-stacked layers. Three of fifteen or 20% of the layers involve corner sharing of oxygens. The structure corresponds directly with one of the two possible 15L close-packed sequences with $R\bar{3}m$ symmetry listed in the "International Tables." That which corresponds has the Zhdanov notation (2)1(1)1.

Eight-Layer Modification

During initial attempts to grow 15L crystals between 1250 and 1350°C in sealed Pt tubes, black hexagonal platelets of another modification were grown. The powder pattern of this phase, given in Table IV, was indexed on the basis of a hexagonal cell with $a = 5.669$ Å and $c = 18.767$ Å. The cell dimensions suggested an 8L stacking sequence which was confirmed by precession photographs. Of the possible space groups $P\bar{6}2c$, $P6_3mc$, and $P6_3/mmc$ the last was chosen, as suggested by the "International Tables" for an 8L sequence. Powder-pattern intensity calculations were made using ideal parameters for the two possible stacking sequences symbolized by the Zhdanov notations /(4)/(4)/ and /1(2(1/1(2)1/. The former contains 75% cubic stacking and, therefore, contains six of eight layers in which corner sharing of octahedra occurs. The stacking sequence may also be symbolized as (ABCABACB). The latter, shown in Fig. 3, contains 25% cubic stacking (ABACACAB sequence) and consequently consists of strings of four face-sharing octahedra linked by corner sharing. Intensity calculations, also given in Table IV, for this structure are in excellent agreement with those observed. Results of calculations for metals only and for metals plus oxygen assuming $Ba_8Mn_8O_{24}$ stoichiometry are given. Structural details will be presented elsewhere.

The determination of structural relations in the $BaMnO_{3-x}$ system provided the important information necessary in locating the stability field of this phase in air. For initial quench runs within the 1300–1350°C range, the 15L phase was used as the

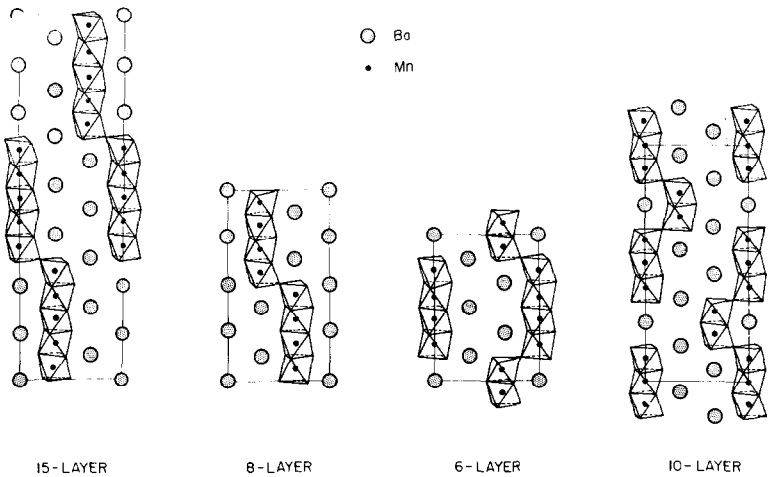

FIG. 3. Cation contents of the hexagonal (110) planes for the various $BaMnO_{3-x}$ modifications stable in air. The two-layer and four-layer modifications (Ref. *8*) are not shown. The structures are idealized.

TABLE IV

X-RAY DIFFRACTION DATA FOR EIGHT-LAYER $BaMnO_{3-x}$

d_{obsd}	d_{calcd}	$h\ k\ l$[a]	I_{obsd}	I^b_{calcd}	I^c_{calcd}
3.864	3.862	1 0 3	8	8	11
3.393	3.392	1 0 4	91	86	95
2.983	2.982	1 0 5	27	18	19
2.835	2.834	1 1 0	100	100	100
2.434	2.434	2 0 1	3	3	<1
2.353	2.353	1 0 7	21	19	17
2.347	2.346	0 0 8	24	19	12
2.285	2.285	2 0 3	6	7	2
2.175	2.175	2 0 4	48	56	25
2.117	2.117	1 0 8	11	9	8
2.055	2.054	2 0 5	13	11	6
1.9190	1.9193	1 0 9	8	8	8
1.8101	1.8105	2 0 7	15	13	8
1.8072	1.8072	1 1 8	12	11	11
1.7257	1.7256	2 1 4	17	20	21
1.6960	1.6960	2 0 8	6	6	4
1.6637	1.6635	2 1 5	6	5	5
1.6367	1.6365	3 0 0	18	16	15
1.6116	1.6116	1,0,11	3	3	2
1.5891	1.5892	2 0 9	5	6	4
1.5256	1.5258	2 1 7	8	8	7
1.4899	1.4901	1,0,12	9	6	6
1.4552	1.4554	2 1 8	3	4	4
1.4172	1.4173	2 2 0	15	15	8
1.3861	1.3862	2 1 9	5	5	4
1.3421	1.3422	3 0 8	3	2	3
1.3190	1.3190	2,0,12	8	7	4
1.3078	1.3077	3 1 4	9	7	7
1.2802	1.2800	3 1 5	3	2	2
1.2133	1.2141 1.2131	3 1 7 2 2 8	5	5	3
1.1956	1.1959	2,1,12	5	5	5
1.1872	1.1874	4 0 4	4	5	2
1.1727	1.1729	0,0,16	2	2	1
1.1393	1.1394	2,1,13	2	2	<1
1.0951	1.0952	3 2 4	4	4	4
1.0836	1.0838	1,1,16	7		
1.0715	1.0714	4 1 0	8		

[a] Indexed on the basis of a hexagonal cell with $a = 5.669$ Å and $c = 18.767$ Å.

[b] Calculated on the basis of an ideal eight-layer stacking sequence of $P6_3/mmc$ symmetry. Atomic positions used are: 2 Ba at (*a*), 2 Ba at (*b*), 4 Ba at (*f*), $z \approx 1/8$; 6 O at (*g*), 6 O at (*h*), 12 O at (*k*), $x \approx 5/6$, $z \approx 1/8$; 4 Mn at (*f*), $z \approx 9/16$, 4 Mn at (*f*), $z \approx 11/16$.

[c] Same as footnote (*b*) but with oxygens excluded.

starting material. A careful inspection of all powder patterns of 15L material heated in this range generally revealed an extra very weak, somewhat broad, line between 26.2 and 26.3° 2θ. Initially this line was thought to represent the metastable formation of small amounts of that phase which exists above 1350°C and which also has a strong line in the same 2θ range. Continued heating of the 15L material, however, causes growth of this line with a corresponding appearance of several new lines and a decrease of 15L line intensities. The new lines match those of the 8L phase previously prepared. Two-layer or higher temperature phases (to be discussed) heated directly within the above temperature range yield 15L material with initially much larger quantities of admixed 8L. Prolonged heating (~2–3 weeks) results in single-phase 8L. It is apparent that 15L converts very sluggishly to 8L and that formation of 8L is enhanced by the use of starting material other than 15L. The strong similarity of the two structures may explain the sluggish transformation and temporary coexistence of both phases. Similar to 15L the 8L does not reverse to 2L but does gain weight when reheated at 1000°C, presumably to stoichiometric $BaMnO_3$. Reversal to 15L also does not occur.

Because of the limited temperature stability range and difficulty of preparation, especially for the large amounts (1.5–2 g) of material required, only one 8L composition was determined gravimetrically (similar to Eq. (2)). The phase existing at 1339°C was found to be $BaMnO_{2.959}$. The pertinent limited range of stoichiometry was inferred from the general slope of the air isobar for other phases and the approximate high- and low-temperature stability limits of juxtaposed phases.

Six-Layer Modification

Above approximately 1350 to near 1475°C a homogeneous, black, modification is stable. Materials quenched from this range readily convert with weight gains to 2L at 1000°C. Stoichiometry determinations were based, therefore, on the reaction

$$(3) \qquad BaMnO_{3-x} + x0 \xrightarrow[\text{air}]{1000^\circ C} \underset{2L}{BaMnO_3}.$$

The transformation is not of true polymorphic or polytypic nature as material sealed in flattened Pt tubes will not convert to 2L at the same temperature. Reversal to 15L and 8L also occurs in air but not in a sealed-tube environment. As shown in Fig. 1, the pertinent range of stoichiometry extends between $x \approx 0.10$ and $x \approx 0.15$. This new modification transforms to all other higher temperature forms.

Unit cell expansion with increasing reduction is slight but nevertheless evident for this form. The diffraction pattern of the phase prepared at 1464°C, given in Table V, was indexed on the basis of a

TABLE V

X-RAY DIFFRACTION DATA FOR SIX-LAYER $BaMnO_{3-x}$

d_{obsd}	d_{calcd}	$h\,k\,l$ [a]	I^b_{obsd}	I^c_{obsd}	I^d_{calcd}	I^e_{calcd}	I^f_{calcd}	I^g_{calcd}
—	4.646	1 0 1	—	—	<1	3	<1	3
4.035	4.035	1 0 2	6	6	7	10	16	24
3.398	3.398	1 0 3	80	60	88	99	53	59
2.863	2.865	1 0 4	25	22	18	17	49	49
2.840	2.841	1 1 0	100	100	100	100	100	100
2.445	2.446	1 0 5	14	12	17	16	15	14
2.425	2.424	2 0 1	2	4	3	<1	3	<1
2.349	2.349	0 0 6	10	12	11	3	11	3
2.324	2.323	2 0 2	3	5	6	2	15	4
2.179	2.180	2 0 3	40	50	57	25	33	15
2.120	2.120	1 0 6	8	8	11	10	0	0
2.017	2.017	2 0 4	10	12	9	5	29	15
1.8639	1.8637	1 0 7	6	5	6	5	7	6
1.8539	1.8538	2 0 5	12	9	12	7	10	6
1.8108	1.8106	1 1 6	6	5	6	8	6	8
—	1.7985	2 1 2	—	—	1	2	3	4
1.7296	1.7295	2 1 3	15	16	21	21	13	13
1.6993	1.6992	2 0 6	9	5	8	5	0	0
—	1.6589	1 0 8	—	—	3	3	9	8
1.6451	1.6450	2 1 4	8	7	6	6	16	16
1.6402	1.6404	3 0 0	16	24	18	17	24	22
1.5577	1.5584	2 0 7	6	3	5	3	5	3
1.5528	1.5526	2 1 5	8	8	8	7	7	6
1.4927	1.4925	1 0 9	5	4	6	6	3	3
1.4583	1.4583	2 1 6	5	5	5	5	0	0
—	1.4326	2 0 8	—	—	3	2	8	5
1.4206	1.4206	2 2 0	15	14	15	8	15	8

[a] Indexed on the basis of a hexagonal cell with $a = 5.683$ Å and $c = 14.096$ Å.

[b] Prepared at 1366°C, air with $a = 5.681$ Å and $c = 14.035$ Å.

[c] Prepared at 1464°C, air and 1430°C in a sealed Pt tube. Cell parameters are given in footnote (*a*).

[d] Calculations based on ideal six-layer sequence with $P\bar{6}m2$ symmetry. Atomic positions used are: 1 Ba in (*a*), 1 Ba in (*d*), 2 Ba in (*h*), $z \approx 1/6$, 2 Ba in (*i*), $z \approx 1/3$; 3 O in (*j*), $x \approx 1/2$, 3 O in (*k*), $x \approx 5/6$, 6 O in (*n*), $x \approx 5/6$, $z \approx 1/6$, 6 O in (*n*), $x \approx 1/6$, $z \approx 1/3$; 2 Mn in (*g*), $z \approx 1/4$, 2 Mn in (*g*), $z \approx 5/12$, 2 Mn in (*i*), $z \approx 1/12$. See Fig. 3, text.

[e] Same as footnote (*d*) but excluding oxygens.

[f] Calculated on the basis of an ideal six-layer $BaTiO_3$-type (Ref. (*4*)) structure, $P6_3/mmc$.

[g] Same as footnote (*f*) but excluding oxygens.

hexagonal cell with $a = 5.683$ Å and $c = 14.096$ Å. Material prepared at 1366°C has $a = 5.681$ Å and $c = 14.035$ Å. Several patterns of the phase show high 2θ angle lines which are somewhat broadened perhaps indicating cell distortion and lower symmetry. This broadening is absent, however, from patterns of material prepared above 1400°C from 2L in sealed Pt tubes and that annealed near 1300°C in sealed tubes. The cell dimensions suggest a six-layer stacking sequence. Single crystals have not been obtained although several heatings of 2L above 1400°C in sealed tubes have produced coarse grained but flakey material which may eventually yield suitable specimens for X-ray analysis.

Initially, because of the 6L sequence and superficial similarity of powder patterns, this phase was thought to be similar to hexagonal, six-layer, $BaTiO_3$ which contains 66 2/3% cubic stacking. As more detailed evidence of phase and structural relations within the $BaMnO_{3-x}$ system unfolded, it became obvious that either the 6L phase was anomalous or that the initially assumed structure was incorrect. Using ideal atomic parameters for a $BaTiO_3$-type stacking ($P6_3/mmc$) and $Ba_6Mn_6O_{18}$ stoichiometry, calculated powder-pattern intensities compared to those observed clearly showed large discrepancies. These could not be reconciled with oxygen deficiency and/or small deviations from the ideal atomic parameters. Disregarding rhombohedral symmetry, the "International Tables" lists two possible configurations for close-packed 6L sequences. The first, /(3)/(3)/ corresponds to hexagonal $BaTiO_3$. The second, /21/12/, has $P\bar{6}m2$ symmetry and an (ABCBCB) sequence with 33 1/3% cubic stacking. Burbank and Evans (*4*) also show this sequence as a possible 6L configuration. The calculated intensities for this structure are in good agreement with those observed. A comparison of calculated and observed intensities is also given in Table V. The proposed ideal structure, shown in Fig. 3, consists of strings of four face-sharing octahedra linked by corner sharing to face-sharing octahedral pairs.

Ten-Layer Modification

Between approximately 1475 and 1550°C another single-phase, black, material exists. Its X-ray powder pattern, given in Table VI, was indexed on the basis of a hexagonal cell with $a = 5.680$ Å and $c = 23.373$ Å. The *c*-axis dimension suggests a ten-layer stacking sequence. Single crystals were obtained from a coarse, irregular-grained (< 0.1 mm) specimen prepared by heating 2L material at 1478°C for 5-days in air. Precession data confirmed the *c*-axis multiplicity and suggested the space groups $P6_3mc$, $P\bar{6}2c$, and $P6_3/mmc$. For a 10L stacking of closest packed layers, the "International Tables" lists three possible sequences for the only suitable space group $P6_3/mmc$. These include /(5)/(5)/ with 80% cubic stacking, /1(3)1/1(3)1/ with 40% cubic stacking, and /2(1)2/2(1)2/ also with 40% cubic stacking. Assuming $Ba_{10}Mn_{10}O_{30}$ stoichiometry and ideal atomic

TABLE VI

X-RAY DIFFRACTION DATA FOR TEN-LAYER $BaMnO_{3-x}$

d_{obsd}	d_{calcd}	$h\ k\ l$[a]	I_{obsd}	I^b_{calcd}	I^c_{calcd}	I^d_{calcd}
4.532	4.534	1 0 2	4	<1	2	4
3.762	3.763	1 0 4	9	24	9	12
3.390	3.388	1 0 5	54	42	74	82
3.054	3.054	1 0 6	14	44	17	18
2.839	2.840	1 1 0	100	100	100	100
2.763	2.763	1 0 7	14	3	6	6
2.512	2.512	1 0 8	17	6	17	16
2.407	2.407	2 0 2	7	1	4	1
2.337	2.337	0,0,10	11	11	12	4
2.297	2.296	1 0 9	6	14	5	5
2.267	2.267	2 0 4	10	18	7	3
2.177	2.177	2 0 5	48	27	48	21
2.112	2.111	1,0,10	5	2	5	5
2.080	2.080	2 0 6	12	27	11	5
1.9807	1.9802	2 0 7	10	2	4	2
1.8816	1.8815	2 0 8	11	4	11	6
1.8364	1.8361	2 1 2	3	<1	<1	<1
1.8108	1.8109	1,0,12	7	3	6	6
1.7862	1.7857	2 0 9	4	9	3	2
1.7720	1.7717	2 1 4	3	5	2	2
1.7278	1.7276	2 1 5	22	10	17	18
1.6941	1.6942	2,0,10	5	1	4	2
1.6780	1.6779	2 1 6	6	13	5	5
1.6397	1.6396	3 0 0	21	16	16	15
1.6248	1.6243	2 1 7	9	1	2	2
1.6076	1.6078	2,0,11	3	6	2	1
1.5686	1.5685	2 1 8	11	3	7	6
1.5270	1.5269	2,0,12	5	2	5	3
1.5114	1.5117	2 1 9	2	6	2	2
1.4856	1.4854	1,0,15	3	3	5	5
1.4550	1.4550	2,1,10	3	<1	3	2
1.4198	1.4200	2 2 0	21	15	15	8
1.3448	1.3448	2,1,12	4	2	4	4
1.3421	1.3423	3,0,10	4	3	4	4
1.3163	1.3163	2,0,15	6	3	6	3
1.3096	1.3096	3 1 5	8	4	6	6
1.2874	1.2876	3 1 6	3	4	2	2
1.2630	1.2629	3 1 7	3	<1	<1	<1
1.2422	1.2422	2,1,14	2	4	2	1
1.2360	1.2361	3 1 8	4	1	3	2
1.2136	1.2136	2,2,10	3	4	4	2
1.2001	1.2001	2,0,17	2	<1	<1	<1
1.1941	1.1942	2,1,15	4	2	4	4
1.1891	1.1893	4 0 5	4	2	4	2
1.1727	1.1727	4 0 6	2	3	1	<1
1.0969	1.0970	3 2 5	4	2	3	3
1.0806	1.0807	1,1,20	3			
1.0734	1.0734	4 1 0	12			

[a] Indexed on the basis of a hexagonal cell with $a = 5.680$ Å and $c = 23.373$ Å.

[b] Calculated on the basis of an ideal ten-layer structure with $P6_3/mmc$ symmetry. Atomic positions used are: 2 Ba at (*c*), 4 Ba at (*e*), $z \approx 3/20$, 4 Ba at (*f*), $z \approx 1/20$; 6 O at (*h*), $x \approx 5/6$, 12 O at (*k*), $x \approx 5/6$, $z \approx 1/20$, 12 O at (*k*), $x \approx 1/2$, $z \approx 3/20$; 2 Mn at (*a*), 4 Mn at (*f*), $z \approx 6/10$, 4 Mn at (*f*), $z \approx 7/10$.

[c] Calculated on the basis of an ideal ten-layer structure with $P6_3/mmc$ symmetry. Atomic positions are: 2 Ba at (*b*), 4 Ba at (*f*), $z \approx 0.15$, 4 Ba at (*f*), $z \approx 0.55$; 6 O at (*h*), $x \approx 1/2$, 12 O at (*k*), $x \approx 1/6$, $z \approx 1/20$, 12 O at (*k*), $x \approx 5/6$, $z \approx 3/20$; 2 Mn at (*a*), 4 Mn at (*e*), $z \approx 1/10$, 4 Mn at (*f*), $z \approx 7/10$. See Figure 3, text.

[d] Same as footnote (*c*) excluding oxygens.

parameters, powder-pattern intensities calculated for the last structure are in good agreement with those observed. Observed versus calculated intensities for the two 40% cubic-stacked structures are compared in Table IV. The proposed ideal structure is shown in Fig. 3. The stacking sequence consists of two sets of three face-sharing octahedral units corner-sharing alternately with two sets of two face-sharing units.

The 10L phase exists in air within the limited range $x \approx 0.175$ and $x \approx 0.20$. Reversal to 15L, 8L, and 6L phases occurs by heating within the appropriate temperature stability field. Ten-layer material similarly heated in a sealed Pt-tube environment will not reverse thus suggesting the lack of true polymorphic or polytypic relations. Conversion to the 2L phase, although accompanied by a weight gain, is incomplete as small amounts of the 15L phase unavoidably develop.

As basic units for the 10L structure are double and triple face-sharing octahedral units, it appears quite possible that during oxidation and conversion to 2L some of the double and triple units may aggregate to form basic 15L units. Any 15L material formed in a random manner would not convert to 2L.

Four-Layer Modification

Above approximately 1550°C, the 10L phase converts to a four-layer modification which exists to at least 1623°C. The powder pattern of this black material has *d*-spacings and line intensities similar to that of 4L $BaMnO_3$ reported by Hardy. Confirmation of symmetry and *c*-axis multiplicity with single crystals, therefore, was not considered necessary. The powder pattern given in Table VII is indexed on the basis of a hexagonal cell with $a = 5.672$ Å and $c = 9.319$ Å. The only possible hexagonal 4L closest packed sequence indicated in the "International Tables" is /(2)/(2)/ with space group $P6_3/mmc$. This corresponds with the structure determined by Hardy. It contains 50% cubic stacking (ABAC sequence) and ideally consists of face-sharing pairs of octahedra linked by corner sharing.

TABLE VII

X-RAY DIFFRACTION DATA FOR FOUR-LAYER $BaMnO_{3-x}$

d_{obsd}	d_{calcd}	$h\ k\ l$[a]	I_{obsd}
4.343	4.345	1 0 1	6
3.380	3.380	1 0 2	68
2.835	2.836	1 1 0	100
2.624	2.625	1 0 3	35
2.374	2.375	2 0 1	6
2.329	2.330	0 0 4	8
2.172	2.172	2 0 2	40
2.105	2.105	1 0 4	4
1.9267	1.9265	2 0 3	16
1.8206	1.8207	2 1 1	2
1.7998	1.8001	1 1 4	4
1.7423	1.7425	1 0 5	4
1.7245	1.7246	2 1 2	12
1.6900	1.6902	2 0 4	4
1.6370	1.6373	3 0 0	12
1.5933	1.5936	2 1 3	13
1.4848	1.4847	2 0 5	5
1.4810	1.4809	1 0 6	7
1.4522	1.4519	2 1 4	4
1.4179	1.4179	2 2 0	13
1.3152	1.3153	2 1 5	3
1.3127	1.3127	2 0 6	6
1.3075	1.3075	3 1 2	6
1.2475	1.2476	3 1 3	6
1.2114	1.2112	2 2 4	4
1.1914	1.1912	2 1 6	4
1.1875	1.1874	4 0 2	6

[a] Indexed on the basis of a hexagonal cell with $a = 5.672$ Å and $c = 9.319$ Å.

When heated within the appropriate temperature stability range, this phase oxidizes and transforms to all lower temperature modifications. Within a sealed-tube environment, no transformation occurs. In air, it exists stably with $x > 0.25$ as determined by oxidation to the 2L form.

Although 4L material was the predominant product from initial experiments above 1550°C, powder patterns generally showed two extra very weak lines near 27.2 and 30.9° 2θ. Intensity of these lines tended to increase with longer heating times and/or higher temperature suggesting the appearance of a second phase (X). The X-ray patterns of specimens partially or totally melted within the 1630–1642°C range showed especially large amounts of this additional phase. Similar lines except near 27.4 and 30.8° 2θ were observed in patterns of 4L material prepared at lower P_{O_2} in vacuum and argon. Again, line intensity tended to increase with prolonged heating. Furthermore, this phase developed more rapidly from small amounts (few milligrams) of material heated in small diameter (2.6 mm i.d.) tubes than from large amounts (0.1 to 0.5 g) in large diameter (4.6 mm i.d.) tubes. It, therefore, became obvious that either (a) the 4L phase decomposes very slowly to an unknown phase represented by the new lines plus manganese oxide, or (b) manganese was being lost through volatility or by soaking into the Pt tubes in air above 1550°C and at lower temperatures at lower P_{O_2}. The experiments detailed in Table I suggest that manganese soaks into the Pt tubes. This drives the bulk composition toward the Ba-rich portion of the system. A powder pattern of phase-X is provided in Table VIII. It can be indexed on the basis of a hexagonal cell with $a = 5.78$ Å and $c = 4.33$ Å. The phase, as indexed, bears a marked similarity to the 2L phase. Curiously, indices with $l > 1$ are not present suggesting a very simple subcell. Further work in the Ba–Mn–O system should elucidate the true nature of this material.

Because of Mn loss, 4L specimens used to measure the weight gains associated with reversal to 2L were prepared in Pt tubes previously soaked with Mn. As this does not necessarily totally insure against Mn loss, the values of x for the 4L phase in Fig. 1 may be subject to slight error.

Negas and Roth (*6*) showed that as 4L $SrMnO_3$ is progressively reduced in air, the lattice expands. Within the limited stoichiometry range for the 4L Ba analogue, cell expansion could not be measured. Similar parameter variations were observed, however, from a number of 4L materials prepared outside of the in-air temperature stability range. Four-layer material, metastably oxidized at 500°C, air, for 25 min, has $a = 5.637$ Å and $c = 9.234$ Å.

TABLE VIII

X-RAY DIFFRACTION DATA FOR UNIDENTIFIED Ba–Mn PHASE[a]

d_{obsd}	d_{calcd}	$h\ k\ l$[b]	I_{obsd}
3.275	3.277	1 0 1	90
2.889	2.891	1 1 0	100
2.503	2.504	2 0 0	10
2.168	2.168	2 0 1	50
1.7354	1.7348	2 1 1	25
1.6695	1.6695	3 0 0	20
1.4463	1.4459	2 2 0	15
1.3235	1.3228	3 1 1	10

[a] Ba/Mn > 1.

[b] Indexed on the basis of a hexagonal cell with $a = 5.78$ Å and $c = 4.33$ Å.

TABLE IX

SUMMARY OF DATA FOR $BaMnO_{3-x}$ PHASES

Phase	Zhdanov symbol	Cubic stacking (%)	Cell dimensions[a] a (Å)	c (Å)	Stability range[b] T (°C)	x in $BaMnO_{3-x}$
2-layer	/(1)/(1)/	0	5.699	4.817	<1150	0.00
15-layer	(2)1(1)1	20	5.681	35.377	1150–1300[c]	0.00(?)–0.02
8-layer	/1(2)1/1(2)1/	25	5.669	18.767	1300–1350[c]	0.03–0.05
6-layer	/21/12/	33 1/3	5.683	14.096	1350–1475	0.10–0.15
10-layer	/2(1)2/2(1)2/	40	5.680	23.373	1475–1550	0.17–0.20
4-layer	/(2)/(2)/	50	5.672	9.319	>1550	>0.25

[a] Hexagonal cells.

[b] In air.

[c] Will not reverse to lower temperature phases after preparation in this range.

Although the extent of oxidation is unknown, cell parameters are considerably smaller than the in-air reduced material. Furthermore, 4L phases, more reduced than in air, were prepared in vacuum at 1250°C (350 μ) and 1345°C (4 μ). Cell parameters are $a = 5.673$ Å, $c = 9.329$ Å, and $a = 5.695$ Å, $c = 9.349$ Å, respectively.

A summary of the $BaMnO_{3-x}$ phases prepared in this study is provided in Table IX.[1]

Other Phase Assemblages

A disc ($1/2 \times 1/8$ in.) of a 1:1 Ba–Mn ratio composition, incompletely reacted at 800 and 1000°C, in-air, and consisting of a multiphase mixture was pressed at ~10 000 psi and heated near 1200°C for 15 hr. The reaction products were the 15L and 2L forms plus an additional phase. The lines of this phase could be indexed on the basis of a hexagonal cell with $a = 5.66$ Å and $c = 20.90$ Å. The c-axis dimension suggests a 9L stacking sequence similar to that reported by Donohue et al. (*9*). As the material could not be prepared in single-phase form, the conditions for its preparation remain unknown. Chamberland et al. (*10*) found that 9L $BaMnO_3$ is a stable high-pressure form, 3 kb/700°C and 65 kb/400–1000°C. It is possible that the highly compacted nature of the starting material in this study was conducive for the metastable development of some 9L material. Although admixed with 15L and 2L, the 9L phase when reheated at 1000°C, air does not reverse to 2L. Analogous with $BaRuO_3$ (*15*), the 9L phase is rhombohedral ($R\bar{3}m$) and consists of strings of three face-sharing octahedra linked by corner-sharing. It corresponds to the only possible sequence, (2)(1), listed in the "International Tables." In a paper to be published later, means other than high pressure of preparing single-phase 9L material will be discussed.

To corroborate the phase relations observed for the 1:1 Ba–Mn ratio, several experiments were conducted using the 1:2 composition. At 1000 to at least 1100°C 2L coexists with an unidentified manganese-rich phase. Material heated at 1253°C consists of 15L plus Mn_3O_4 while that at 1366°C is 6L plus Mn_3O_4. When heated at 1442°C partial melting occurred. The quench products are 6L + Mn_3O_4. Higher temperature experiments were terminated because of melting. In vacuum, 150 μ (1325°C) and 4 μ (1345°C), reduced 4L phases were found to coexist with MnO. At the 1:6 ratio the manganese-

[1] After completion of this manuscript, Dr. B. Fender of the Inorganic Chemistry Laboratory, Oxford University, discussed and provided the writers with a copy of a recent (March 1969) unpublished dissertation, "Thermodynamic Properties of Mixed Metal Oxides," by J. R. Greaves. A limited number of experiments were conducted involving the system $BaMnO_x$. Using high purity $BaCO_3$ and Mn_3O_4 as starting materials, stoichiometric $BaMnO_3$ was prepared and found to exist to at least 1100°C in air. An inspection of the X-ray powder data for this phase suggests that all reflections can be indexed on the basis of a two-layer structure identical to that reported in this study. A specimen heated for 2 days at 1250°C in air was found to have the composition $BaMnO_{2.98}$. A satisfactory indexing of its powder pattern could not be found. The composition of the 15-layer phase at 1250°C in this study is near $BaMnO_{2.988}$. An inspection of the powder data reported by Greaves suggests at least a mixture of the 2-layer and 15-layer phases. Higher temperature experiments were not conducted. At 1040°C and 10^{-4} Torr, a phase of $BaMnO_{2.743}$ composition was prepared. The d spacings and line intensities of the reported powder pattern can be reconciled with the 4-layer structure. Four-layer material with a composition near $BaMnO_{2.75}$ is reported in this study to form above 1550°C in air or at lower temperatures in vacuum or argon. The data of Greaves and that of this study are in particularly good accord.

rich phase coexists with Mn_3O_4 within the 1000–1100°C range in air.

Stoichiometry-Structural Relations

A simple structural pattern exists among the $BaMnO_{3-x}$ phases as shown in Fig. 3 and Table IX. Considering only the number of face-sharing octahedra the following scheme is evident:

$$2L(\text{infinite}) \rightarrow 15L(5) \rightarrow 8L(4) \rightarrow 6L(4\ \&\ 2) \rightarrow 10L(3\ \&\ 2) \rightarrow 4L(2)$$

The maximum number of face-sharing octahedra in a given sequence (parenthetically enclosed) progressively decreases with increasing temperature.

A plot of c/N versus (%) cubic stacking, shown in Fig. 4, provides some interesting features. A similar diagram is obtained when based on a c/a ratio per layer (N) versus (%) cubic stacking. The variable c/N represents, for any given structure, the "average thickness" of the BaO_3 layers between which space is provided for Mn cations. A general decrease of c/N with increasing cubic stacking (%) is evident, as expected. The decrease appears linear from 2L → 15L → 8L. The reported value for 9L $BaMnO_3$ also lies on the same line. Significantly, these four phases are either stoichiometric (2L and 9L) or can exist both in slightly anion deficient and fully oxidized configurations. If the straight line is extrapolated to 50% cubic stacking, an average layer thickness of 2.28–2.29 Å is derived for a stoichiometric 4L $BaMnO_3$. As it is well-known that the stability of cubic stacking is enhanced by hydrostatic pressure, it may be possible to stabilize this form at elevated pressures. Pressures higher than those reported for the preparation of 9L $BaMnO_3$ (3–65 kb) would be necessary.[2]

Increased (%) cubic stacking also appears to occur over a rather limited range of c/N values. The most anion-deficient, reversible, phases, 6L, 10L, and 4L are members of this group. Where measurable, variation of layer thickness for a given phase is shown. The c/N (or c/aN) values for this series deviate markedly from the established "stoichiometric series" line. In Fig. 4, the direction of increasing temperature and/or reduction is indicated by horizontal arrows while diagonal arrows depict the transformations as a function of increasing

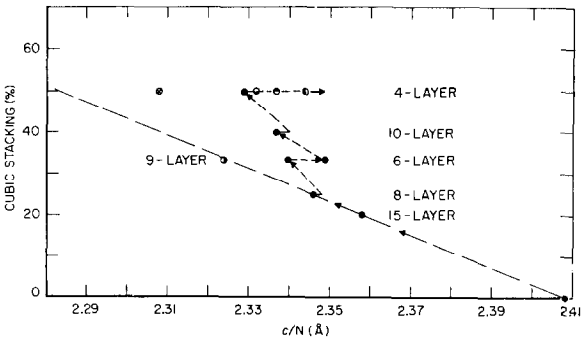

FIG. 4. Plot of (%) cubic stacking versus c/N (N = number of BaO_3 layers per cell) for $BaMnO_{3-x}$ modifications. At zero (%) cubic stacking the two-layer phase exists. Diagonal arrows represent phase transitions with increasing temperature. Horizontal arrows depict the c/N variation for a given phase as a function of increasing temperature and/or anion deficiency. ◒, ◓ Prepared in vacuum, this study; ⊗, reduced four-layer material metastably reoxidized, 500°C, air; ◐, four-layer material (Ref. *8*); ◑, nine-layer $BaMnO_3$ (Ref. *9*).

temperature. Clearly, stabilization of cubic stacking is related to the reduction process. This also occurs in the system $SrMnO_{3-x}$ (*6*). This phenomenon does not violate well-established crystal-chemistry principles nor does it contradict the hydrostatic pressure considerations. With increasing temperature, phases with progressively decreasing anion content are stabilized even though increases in cubic stacking (%) occur. As the phases are not of fixed stoichiometry, they are not related by polymorphism or true polytypism. Furthermore, the basic structural units depicted in Fig. 3 are octahedra in accordance with a continuous, nondisturbed, oxygen network. Because of stoichiometry imposed requirements, some of the Mn must assume a lower coordination number. The structures, therefore, consist of mixed types of transition metal-oxygen polyhedra. Wadsley (*17*) has discussed extensively the importance of such schemes. Tetravalent Mn is known in oxide chemistry to be compatible primarily with octahedral coordination. The trivalent state is consistent with octahedral and trigonal bipyramid sites (*18*) but not with tetrahedral or square planar. Thus when $BaMnO_3$ is reduced, Mn can accommodate the anion loss by assuming a permissible lower coordination number without gross structural rearrangement. Two of the possible localized environments which may result in a close-packed structure are illustrated in Fig. 5. If an A-layer (cubic-type) oxygen is removed, the corner sharing of octahedra is disrupted. Similarly, if a hexagonal-type layer (B,C) anion is missing, face

[2] During the process of publication, a paper by Syono et al. (*16*) was brought to our attention. Four-layer $BaMnO_3$ having a c/N value between 2.31–2.32 Å was prepared above 90 kb and 1200°C. Furthermore, the 4L form reported by Hardy (*8*) could not be prepared under atmospheric conditions at 1350°C.

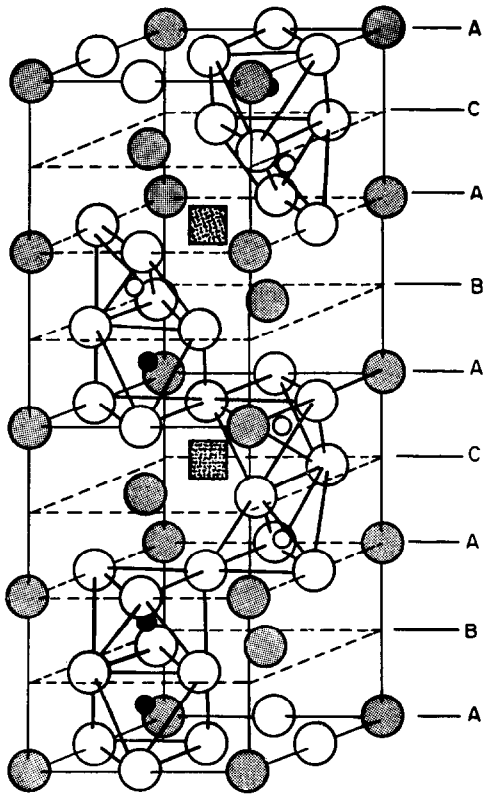

FIG. 5. Possible environments about manganese in a close-packed structure as a result of (a) a vacant A-layer anion position and (b) a vacant C- (or B-) layer anion position. Large shaded circles are Ba; large open circles are oxygen; small dark circles are Mn^{4+}; small open circles are Mn^{3+}; shaded squares are vacant oxygen positions. Polyhedra are shown without distortion.

sharing is disrupted. Assuming a slight displacement of the transition metal, the first case results in two, nonbriding, Mn^{3+}-trigonal bipyramids each sharing a common face with a Mn^{4+} octahedron. The second example creates two edge-sharing trigonal bipyramids.

Phase transitions involving an increase in the amount of cubic stacking in XYO_3 compounds can be induced by increasing pressure. This is accomplished by the disruption of face-sharing octahedral sequences. As face-sharing metal–metal distances for a given phase are progressively decreased, the electrostatic repulsion term begins to dominate. Ultimately, phase stabilization is possible only through a transformation involving an increase in the amount of corner sharing. Shorter face-sharing metal distances are avoided while the average layer thickness decreases. This general effect is simulated under atmospheric pressure by (a) decreasing the effective size of the X cation while maintaining the Y transition metal and (b) increasing the effective radius of the Y metal while maintaining the X cation constant. The series $Ba_{1-x}Sr_xRuO_3$ (*19*) illustrates (a). Method (b) is suggested by the pairs $SrMnO_3$(4L)–$SrRuO_3$ (perovskite) and $BaMnO_3$(2L)–$BaRuO_3$(9L). As the effective radius increases from 0.54 to 0.62 Å (*20*) from Mn^{4+} through Ru^{4+}, the metals avoid short face-sharing distances by increasing the amount of corner sharing.

To account for the observed transformations of the $BaMnO_{3-x}$ phases, it is proposed that reduction is accompanied structurally by the formation of coordination schemes similar to those in Fig. 5. The introduction of increasing amounts of the larger Mn^{3+} cation [radius = 0.58 Å(20)] causes structural expansion as suggested by the positive deviations of c/N and c/aN from their ideal values. This is evident especially for the most reduced phases. Concomitant disruption of face sharing and/or corner sharing through anion loss is an influencing factor in preventing the effective screening of not only the larger Mn^{3+} but the remaining Mn^{4+} cations. The situation is, therefore, nearly analogous with case (b) discussed above. For $BaMnO_{3-x}$ phases, however, cubic stacking is favored not by replacing the Mn with a different, larger, cation but by increasing the effective radius of the Mn itself through reduction.

The data suggest that the long face-sharing sequences cannot tolerate large Mn^{3+} concentrations. The 2L, 15L, and 8L forms show only very limited homogeneity ranges. This perhaps reflects a sensitivity toward mixed Mn^{4+}–Mn^{3+} face-sharing units. In contrast, the limiting stoichiometries for the 6L and 10L forms are near $Ba_6Mn_4^{4+}Mn_2^{3+}O_{17}$ and $Ba_{10}Mn_6^{4+}Mn_4^{3+}O_{28}$, respectively. Here the number of Mn^{3+} cations is equivalent to the number of Mn positions available in the double polyhedral units of each structure. This would permit all remaining Mn^{4+} to order within the long face-sharing sequences. Furthermore, corner sharing need not be disrupted as missing anions could be associated with the double polyhedral units such that pairs of edge-sharing trigonal bipyramids develop. Continued oxygen loss must affect the remaining face-sharing sequences since removal of anions from the trigonal bipyramid units would necessarily cause unsatisfactory Mn coordination schemes. As the longer sequences are unstable with respect to limited amounts of Mn^{3+}, phase instability and transformation result. Each transition, therefore, involves a maximization of corner sharing by the formation of shorter face-sharing sequences. Short metal–metal

distances and the possible face sharing of Mn^{3+}–Mn^{4+} polyhedra are also avoided.

Significantly, the c/N or c/aN for the 9L form is never attained. This undoubtedly reflects the influence of Mn^{3+} formation and anion loss in preventing the development of an effective metal separation necessary for phase stabilization. The 6L structure, therefore, is the alternative at $33\frac{1}{3}\%$ cubic stacking.

References

1. L. KATZ AND R. WARD, *Inorg. Chem.* **3**, 205 (1964).
2. "International Tables for X-ray Crystallography," Vol. II, p. 342, Kynoch Press, Birmingham, 1959.
3. J. J. LANDER, *Acta Crystallogr.* **4**, 148 (1951).
4. R. D. BURBANK AND H. T. EVANS, *Acta Crystallogr.* **1**, 330 (1948).
5. T. NEGAS, R. S. ROTH, AND J. L. WARING, *Abstr. 108, Inorg. Chem. Div., Amer. Chem. Soc., 156th National Meeting* (1968).
6. T. NEGAS AND R. S. ROTH, *J. Solid State Chem.* **1**, 409 (1970).
7. B. E. GUSHEE, L. KATZ, AND R. WARD, *J. Amer. Chem. Soc.* **79**, 5601 (1957).
8. A. HARDY, *Acta Crystallogr.* **15**, 179 (1962).
9. P. C. DONOHUE, L. KATZ, AND R. WARD, *Inorg. Chem.* **5**, 339 (1966).
10. B. L. CHAMBERLAND, A. W. SLEIGHT, AND J. F. WEIHER, *J. Solid State Chem.* **1**, 506 (1970).
11. "X-ray 67, Program System for X-ray Crystallography," Technical Report 67-58, Univ. of Maryland, Computer Science Center, 1967.
12. D. K. SMITH (modified by E. H. Evans), A Revised Program for Calculating X-Ray Powder Diffraction Patterns, UCRL 50264, Univ. of Calif., Lawrence Radiation Laboratory, Livermore, Calif., 1967.
13. F. JELLINEK, *Inorg. Nucl. Chem.* **13**, 329 (1960).
14. W. H. ZACHARIASEN, *Acta Crystallogr.* **1**, 263 (1946).
15. P. C. DONOHUE, L. KATZ, AND R. WARD, *Inorg. Chem.* **4**, 306 (1965).
16. Y. SYONO, S. AKIMOTO, AND K. KOTO, *J. Phys. Soc. Jap.* **26**, 993 (1969).
17. A. D. WADSLEY, in *Non-Stoichiom. Compounds* (1964).
18. J. B. GOODENOUGH AND J. M. LONGO, "Crystallographic and Magnetic Properties of Perovskite and Perovskite Related Compounds," Landolt-Bornstein Tabellen Neue Serie III/4a, Springer-Verlag, Berlin, 1970.
19. J. M. LONGO AND J. A. KAFALAS, *Mater. Res. Bull.* **3**, 687 (1968).
20. R. D. SHANNON AND C. T. PREWITT, *Acta Crystallogr. Sect. B* **25**, 925 (1969).